Plant, Cell & Environment

WILEY

Plant, Cell & Environment

ORIGINAL ARTICLE OPEN ACCESS

Extreme Polyploidy Reveals Functional Trade-Offs in Plant Drought Responses

Javier López-Jurado[1,2,3] | Enrique Mateos-Naranjo[2] | Francisco Balao[2] | Ajaree Thonglim[4] | Frederic Lens[4,5] | Timothy J. Brodribb[1]

[1]School of Natural Sciences, University of Tasmania, Hobart, Australia | [2]Departamento de Biología Vegetal y Ecología, Facultad de Biología, Universidad de Sevilla, Sevilla, Spain | [3]Departamento de Botánica, Ecología y Fisiología Vegetal, Universidad de La Laguna, Laguna, Spain | [4]Naturalis Biodiversity Center, Research Group Functional Traits, Leiden, the Netherlands | [5]Leiden University, Institute of Biology Leiden, Plant Sciences, Leiden, the Netherlands

Correspondence: Javier López-Jurado (javlopez@us.es)

Received: 14 April 2026 | **Revised:** 15 June 2026 | **Accepted:** 15 July 2026

Funding: Universidad de Sevilla; Australian Research Council Centre of Excellence for Plant Success in Nature and Agriculture; Ministerio de Ciencia e Innovación

Keywords: cell size coordination | drought survival | hydraulic vulnerability | minimum conductance | polyploidy | xylem anatomy

ABSTRACT

Polyploidy shapes plant physiology and anatomy, yet the extent to which different ploidy levels influence drought responses remains unclear. Here, we investigated how ploidy affects cell-level coordination and functional traits associated with water transport and retention. We used glasshouse-grown plants of the carnation *Dianthus broteri*, a species complex composed of naturally distinct populations differing in cytotype: diploid (2×), low-polyploid (4×), and high-polyploid (6× and 12×). Leaf anatomical traits scaled with ploidy: higher-ploidy cytotypes exhibited larger stomata and pavement cells, with coordinated reductions in stomatal and vein densities. However, the 12× cytotype deviated from this trend and displayed higher g_{min} and thinner epicuticular wax. Stem xylem anatomical traits and hydraulic vulnerability were largely conserved, except for thicker intervessel pit membranes in 6× and 12× individuals, which correlated with delayed embolism spread (P_{25}). Plant structure–function trait combinations indicate that cytotypes differ in water-use syndromes rather than aligning along a single dimension of drought response. Under drought conditions, lower ploidies maintained functional canopies through reduced water loss, whereas 12× showed a less conservative water-use strategy and seasonal canopy loss. Altogether, we provide new insights into how polyploidy can influence drought adaptation and survival strategies via anatomical and functional trait shifts.

1 | Introduction

Ploidy, referring to the number of full chromosome sets in an organism, is a key factor influencing phenotype. Across the tree of life, plants are particularly prone to whole-genome duplications (WGD; Otto and Whitton 2000; Zhang et al. 2020), which often give rise to polyploid lineages (i.e., organisms with more than two sets of chromosomes; Wood et al. 2009; Barker et al. 2016). The genomic, physiological, developmental, and reproductive changes associated with polyploidy are known to contribute to the evolutionary success of many plant lineages (Soltis and Soltis 2016; Van De Peer et al. 2017). However, evidence suggests that trait evolution following WGD is shaped by a complex interplay between short- and long-term effects (Bomblies 2020), which complicates efforts to predict evolutionary outcomes. The direction and magnitude of polyploid divergence from diploids likely depend on complex regulatory networks (Ebadi et al. 2023) as well as contextual factors such as environmental conditions (i.e., differing selective pressures) and the timing of polyploid origins.

The last two authors share the joint senior authorship.

Among closely related taxa, ploidy often covaries with genome size, which in turn scales predictably with cell size (Šímová and Herben 2012; Roddy et al. 2020). The relatively consistent WGD-driven *gigas* effect—where polyploids tend to exhibit larger cells than their diploid relatives (Stebbins 1971)—can, however, vary among cell types (Katagiri et al. 2016). This reflects the influence of polyploid regulatory complexity on developmental and anatomical coordination. Furthermore, empirical comparisons are often restricted to diploids and their immediate lower-order polyploid descendants (e.g., 3× or 4×), neglecting higher-order polyploids (> 4×). The latter polyploids, shaped by multiple rounds of genome duplication, may possess even greater potential for evolving complex phenotypic novelties. This opens an important research avenue into whether repeated genome duplication can generate extreme or previously inaccessible phenotypes, as it may promote trait uncoupling (e.g., Balao et al. 2011; López-Jurado et al. 2022) and expand the boundaries of trait space (Messier et al. 2017). In leaves, this degree of trait coordination is particularly important as it underpins whole-plant water and carbon relations (Brodribb et al. 2013; Brodribb et al. 2017). Plants with higher gas exchange rates lose more water through transpiration and require a more efficient vascular system to sustain root-to-shoot water transport (Brodribb and Feild 2000; McKown et al. 2010; Manzoni et al. 2013), leading to critical functional covariation between stomata and veins (Brodribb et al. 2017).

The capacity of polyploids to achieve novel trait values and combinations helps explain why they have been observed to exhibit both increased stress tolerance (Van De Peer et al. 2021; Tossi et al. 2022) and enhanced productivity (Greer et al. 2018; Trojak-Goluch et al. 2021). In this context, the study of hydraulic traits is essential, as they govern both water transport and carbon assimilation. What is known is that polyploids often show wider xylem vessels than diploids—linked to the *gigas* effect (Barceló-Anguiano et al. 2021; Losada et al. 2023)—which theoretically increases hydraulic conductance, according to the Hagen–Poiseuille equation (Zimmermann 1983). However, empirical findings are inconsistent. For instance, polyploids showed much higher hydraulic conductance than diploids in *Chamerion angustifolium* (Maherali et al. 2009), a herbaceous perennial from temperate environments, while the opposite pattern was reported in *Atriplex canescens*, an evergreen shrub from arid and semi-arid regions (Hao et al. 2013). In turn, the lower conductance in *A. canescens* polyploids was accompanied by increased embolism resistance (Hao et al. 2013), whereas in *C. angustifolium*, greater conductance was observed alongside similar embolism vulnerability between ploidy levels (Maherali et al. 2009). These results across species with different growth forms and from contrasting environments indicate that the relationship between ploidy and hydraulic traits can vary, which may contribute to greater variability in the classic hydraulic efficiency–safety trade-off (Gleason et al. 2016; Grossiord et al. 2020; Yan et al. 2020). This added complexity likely originates from unpredictable variation in certain commonly measured xylem anatomical traits, such as vessel diameter, which has shown ambiguous associations with embolism resistance across different lineages (Lens et al. 2022, 2023).

Under stress, particularly drought, acquiring sufficient embolism resistance is a key adaptation for plant survival (Blackman et al. 2010; Lens et al. 2013; Shao et al. 2023). This is especially relevant given the reported tendency of polyploids to colonise environmentally extreme habitats (Rice et al. 2019; Folk et al. 2020). Polyploids may also rely on other strategies to cope with stress, such as increasing tissue water storage (Preisler et al. 2022; Pacey et al. 2022), reducing water loss via finer stomatal control (Martin-StPaul et al. 2017), or having less permeable cuticles under high evaporative demand (Duursma et al. 2019; Slot et al. 2021). However, the extent to which these responses are specifically associated with polyploidy remains uncertain. At a broader scale, polyploidy may even shift a species' ecological strategy (López-Jurado et al. 2022)—for example, favouring drought survival over drought resistance, particularly in perennials (Volaire 2018). In addition, plant survival can be enhanced not only by maintaining function during drought, but also by strategic reductions in growth or photosynthesis to conserve carbon (McDowell et al. 2008; Bielenberg 2011), or even by early senescence to reduce leaf surface area and water loss (Schippers et al. 2015). In all cases, the context-dependent nature of trait evolution in polyploids and the wide array of mechanisms underlying plants' drought tolerance explain the lack of consistent patterns in climatic niche differentiation between diploids and polyploids (Meirmans and Kolář 2025).

In this study, we used *Dianthus broteri* (Caryophyllaceae) as a perennial model species to investigate how ploidy shapes leaf cell coordination and drought-adaptive strategies. *D. broteri* is a subshrub autopolyploid species complex endemic to the Iberian Peninsula, comprising four ploidy levels (2×, 4×, 6×, and 12×; Balao et al. 2009). Available reproductive data indicate that *D. broteri* individuals are self-compatible but predominantly outcrossing, with pollinator-mediated reproduction documented in detail for the 12× (Balao et al. 2024) and field observations for the remaining ploidy levels. No natural hybridisation has been observed among these cytotypes, and previous work supports their treatment as genetically and ecologically differentiated evolutionary units (Balao et al. 2010). Genome size scales consistently with ploidy across cytotypes, with a roughly six-fold increase in DNA content from 2× to 12× (Balao et al. 2009). Lower ploidies (2× and 4×) occur in areas with moderate annual rainfall and summer temperatures, whereas 6× and 12× are associated with lower water availability and warmer summers. Within this group, 6× populations are found in regions with the lowest annual precipitation, and 12× experience the highest atmospheric evaporative demand (López-Jurado et al. 2019a; Table S1). These contrasting environmental conditions suggest that cytotypes have been exposed to different selective pressures. In this context, the previously reported decoupling of morphological traits (floral and vegetative; Balao et al. 2011) and resource-use traits (López-Jurado et al. 2022) in *D. broteri* raises the possibility that repeated genome duplication may facilitate the evolution of alternative functional trait combinations that are less constrained by typical scaling relationships. More recently, higher-ploidy *D. broteri* individuals were found to exhibit increased stomatal conductance and hydraulic efficiency compared with lower ploidies (López-Jurado et al. 2025b). However, the drought responses of these 2× to 12× cytotypes, particularly their hydraulic safety and water loss control, have not yet been explicitly tested.

In line with the rationale outlined above, we aimed to evaluate whether polyploidy facilitates greater gas exchange and water supply capacity while maintaining similar or even higher thresholds of embolism vulnerability. We hypothesised that this potential functional advantage in polyploids would be underpinned by anatomical adjustments in both leaf and stem tissues that deviate from expected genome-size scaling relationships. Overall, we predicted that different ploidy levels would display contrasting whole-plant drought responses. In particular, we expected higher ploidy levels to be characterised by shifts in the coordination between traits related to water supply and water loss. These shifts may help explain their occurrence in more extreme environments as a result of both polyploidy and environmental selection.

2 | Materials and Methods

2.1 | Plant Material and Sampling Design

Plants from the four ploidy levels of *Dianthus broteri* were obtained from seeds collected from seven to ten individuals across three natural populations per cytotype (Table S1). Each cytotype was therefore represented by multiple independent open-pollinated maternal lines spanning its geographic distribution, rather than by a single genotype or by progeny from a single mother plant. Hydraulic vulnerability and xylem anatomy were measured on 6-month-old individuals derived from these maternal lines, ensuring a comparable developmental stage and a shared maternal genetic origin within each cytotype. Leaf anatomical traits and the remaining physiological measurements were assessed on 1-year-old individuals representing multiple maternal lines per cytotype. Within each experimental set, sampled leaves were healthy, fully expanded, and mature, and were taken from comparable nodal positions within the canopy (mid-canopy leaves).

All plants were grown from germination under identical glasshouse conditions: day/night temperatures of 25/21°C, relative humidity between 40% and 60% and unfiltered natural light (ranging from 200 μmol photons $m^{-2} s^{-1}$ to 1200 μmol photons $m^{-2} s^{-1}$ during the day). Plants were cultivated in 2.5-L pots filled with a 3:1 mixture of potting substrate (composed of composted fine pine bark and coarse-washed river sand) and perlite. Experiments were conducted at either the University of Tasmania (leaf epidermal anatomy, vein density, and drought experiments) or Naturalis Biodiversity Center (stem hydraulic vulnerability and xylem anatomy). Pots were watered daily to prevent premature xylem embolism formation before hydraulic vulnerability and drought experiments, as well as during the measurement of all anatomical traits (Table 1).

2.2 | Leaf Epidermal Anatomy and Vein Density

Fully mature leaves of *D. broteri* were detached from three 1-year-old individuals per ploidy level, grown at the University of Tasmania. In the lab, they were cut into 1 cm^2 squares under a stereomicroscope using a handheld razor blade and soaked in commercial household bleach (50 g L^{-1} sodium hypochlorite and 13 g L^{-1} sodium hydroxide) to clear the tissue. Bleach was removed by washing, and the inner leaf contents were brushed off, leaving epidermal peels with the cuticle attached. Epidermal preparations from the adaxial surface were then stained with dilute (< 0.1%) crystal violet to enhance contrast of cell outlines, rinsed, and mounted on microscope slides in phenol glycerine jelly. Digital photomicrographs of at least three fields of view per preparation were taken using an Eclipse 50i microscope (Nikon, Tokyo, Japan) at ×100 magnification. The images were subsequently analysed using the EPIDERMALMORPH R package (Brown and Jordan 2023), which enabled the quantification of multiple informative leaf epidermal traits, including stomatal and pavement cell area and stomatal density (Table 1).

For vein density measurements, a second set of mature leaves of comparable developmental stage was sampled from the same *D. broteri* individuals. Paradermal sections were obtained under a stereomicroscope by carefully removing the adaxial epidermis and palisade layer with a handheld razor blade. The sections were then cleared in commercial household bleach and stained with diluted (< 0.1%) toluidine blue to highlight lignin-rich

TABLE 1 | Leaf and Stem Anatomical Traits Included in This Study, With Their Acronyms, Definitions, and Calculation Methods.

Acronym	Definition	Calculation
—	Stomatal area	Surface area of an individual leaf stomata
—	Stomatal density	Number of stomata per unit leaf area
—	Pavement cell area	Surface area of an individual leaf epidermal pavement cell
—	Vein density	Total length of veins per unit leaf area
T_{EW}	Leaf epicuticular wax thickness	Thickness of the epicuticular wax layer on the adaxial leaf surface
A_{VL}	Vessel lumen area	Area of an individual xylem vessel lumen in cross-section, measured directly from thresholded images
T_V	Vessel wall thickness	Thickness of an individual vessel wall
$(T_{VW}/D_{MAX})^2$	Theoretical vessel implosion resistance	Square of double intervessel wall thickness divided by the maximum diameter of the largest vessel
V_G	Vessel grouping index	Ratio of the total number of vessels to the total number of vessel groupings (including solitary and grouped vessels)
T_{PM}	Intervessel pit membrane thickness	Thickness of the intervessel pit membrane measured at its thickest point

veins. After sufficient rinsing, the preparations were mounted in phenol glycerine jelly and photographed using the same Eclipse 50i microscope at ×100 magnification. Vein density was determined as the total length of leaf vascular tissue per unit leaf area using ImageJ (Schneider et al. 2012).

The leaf epidermis was further characterised by measuring the thickness of the epicuticular wax layer on the adaxial surface (T_{EW}; Table 1). Fully mature leaves were again sampled from three 1-year-old individuals per ploidy level. A mid-leaf segment was embedded in corn syrup solution and oriented perpendicular to the cutting plane. Transverse sections (10–20 μm thick) were obtained using a freeze microtome, stained with a dilute solution (< 0.1%) of toluidine blue, rinsed in water, and mounted in glycerol jelly. Samples were then imaged at 40× magnification using a Zeiss Axio Imager.M2 compound microscope equipped with an AxioCam MRc5 digital camera (Carl Zeiss). Images were analysed using ImageJ (Schneider et al. 2012).

2.3 | Minimum Leaf Conductance and Phase Transition Temperature

Water conservation during drought is crucial to delaying dehydration injury and, therefore, defining drought adaptation strategies. We assessed this by quantifying residual water loss through the leaves following stomatal closure, expressed as minimum leaf conductance to water vapour (g_{min}). g_{min} was measured at six different temperatures, from 25°C to 45°C in 4°C increments: 25, 29, 33, 37, 41, and 45°C.

At each temperature point, seven leaves were sampled from seven 1-year-old individuals per ploidy level, all grown in the University of Tasmania glasshouse. Leaves were excised, placed in bags with a saturated atmosphere, and their cut bases sealed in the lab using paraffin wax. Before each dehydration experiment, leaves were scanned and their area measured using ImageJ (Schneider et al. 2012).

Leaves were then gently hung using pegs from the trays of a temperature-controlled dehydrating oven, equipped with a fan running to reduce boundary layer resistance. The oven was set to the target temperature for each measurement. Changes in leaf mass were recorded every 20–30 min using a precision balance (Mettler Toledo, resolution = 0.1 mg, Model MS204S, Port Melbourne, VIC, Australia). During weighing, samples were briefly removed from the oven. Measurements continued until the rate of water loss reached a steady state, indicating stomatal closure. Afterwards, leaves were dried at 60°C for 72 h to determine dry mass.

Changes in leaf weight between timepoints were used to calculate water loss. The transpiration rate (R) was derived from changes in water mass in the leaf (w) over time (t), divided by the total leaf area (A):

$$R = \Delta w/(\Delta t \times A)$$

Here, A corresponds to the double-sided area, as leaves of *D. broteri* are amphistomatic. This slope (R) was then used to calculate g_{min} based on the vapour pressure deficit (VPD). VPD was estimated using the Arden Buck equation (Buck 1981) from temperature and relative humidity measured by a data logger (HOBO model MX2302A; Onset Computer Corporation, Bourne, MA, USA) placed inside the oven.

Values of g_{min} for each ploidy level and temperature were modelled using the *segmented* package in R (Muggeo 2008) to identify a single breakpoint in the g_{min}–temperature relationship. This was used to determine the phase transition temperature (T_p), the point at which g_{min} begins to increase rapidly.

2.4 | Optical Vulnerability Technique

2.4.1 | *Image Capture*

Xylem vulnerability was quantified by visually recording embolism in mature basal stems, specifically in the portion just above the soil. Prior to vulnerability measurements, plants were transferred to a dark room for *c.* 1 h to allow for water potential equilibration. Plants were taken out of their pots, and roots were thoroughly washed to remove most of the soil before being covered with a wet paper towel. This was done to accelerate the dehydration process, so plants could progress from full hydration to death within *c.* 5 d. The entire monitoring was conducted in darkness to avoid affecting the captured images, with only overhead illumination (using white light-emitting diodes) directed at the monitored stems.

Three 6-month-old plants per ploidy level of *D. broteri* were selected for optical visualisation of embolism in stems. These individuals, grown at Naturalis Biodiversity Center, had fully expanded, mature leaves at the time of measurement. First, a thin layer of peripheral tissues surrounding the xylem was cut longitudinally and removed under a stereomicroscope using a flexible razor blade, improving xylem exposure and providing a clearer view of the embolism events. Previously performed cross-sections facilitated this process by ascertaining the optimal amount of tissue to remove without damaging xylem vessels in the wood cylinder. The exposed xylem was covered with hydrogel (Tensive Gel; Parker Laboratories Inc., Fairfield, NJ, USA) prior to measurements to slow down evaporative water loss.

The monitored stem parts were fixed onto a rectangular piece of glass using black tape to prevent distortion during drying. Photographs were taken at ×5 magnification every 90 s using a Nikon D700 camera (Nikon Corporation, Tokyo, Japan) mounted on the ocular of a Wild M3 stereomicroscope (Leica Microsystems, Wetzlar, Germany). Image collection continued until no embolism events were detected for at least 12 h, at which point embolism was considered to have reached 100% of xylem conduits.

2.4.2 | *Plant Water Potential*

Plant water potential (Ψ) was measured using a Scholander-type pressure chamber (PMS Instruments, Albany, OR, USA) on non-transpiring leaves adjacent to the monitored stem, following the recommendations of Rodriguez-Dominguez et al. (2022). Ψ measurements were taken every 8 h until all

monitored xylem conduits were fully embolized. Linear regressions of Ψ against time showed a strong fit ($R^2 > 0.92$; $p < 0.05$) across all plants, regardless of ploidy level. This approach allowed for the generation of continuous Ψ data throughout the measurement period. Given the experimental conditions—plants disconnected from soil and closed stomata during dehydration—hydraulic disequilibrium between tissues was not expected, at least until significant embolism events could compartmentalise plant organs. For this reason, stems were occasionally used to measure Ψ when leaves could not be properly sealed in the compression gland gaskets, causing gas leaks.

2.4.3 | *Image Analysis*

Xylem embolism was detected by tracking changes in light transmission through the stem, which reflect the transition of water-filled conduits into air-filled (embolized) vessels. These transitions appear in the images as localised changes in pixel intensity and were used to quantify the progression of embolism over time (Brodribb et al. 2016). Embolism events were identified by frame-to-frame pixel differencing, and the cumulative affected xylem area was expressed as a proportion of the exposed xylem area. Image stacks for each monitored plant were analysed in ImageJ (Schneider et al. 2012) following the instructions from http://www.opensourceov.org/. The resulting percentage embolism was plotted against predicted Ψ to construct vulnerability curves. The water potentials at 25% and 50% cavitated xylem (P_{25} and P_{50}, respectively) were extracted for each monitored individual. A unique stem vulnerability curve was produced for each *D. broteri* ploidy by pooling the data from the three individuals and fitting a 'Weibull' model using the *fitplc* package in R (Duursma and Choat 2017).

2.5 | Xylem Anatomy

2.5.1 | *Light Microscopy (LM)*

Stems were collected from three 6-month-old, well-watered *D. broteri* individuals per ploidy, grown from seeds of the same mother plants used in the optical vulnerability technique, to match anatomical traits with hydraulic vulnerability. Basal stem segments, sampled just above the soil surface and approximately 8 mm in length, were sectioned without embedding using a Reichert sliding microtome (Reichert, Vienna, Austria). Sections were then bleached with sodium hypochlorite and stained with a safranin–alcian blue mixture (35:65). Safranin was prepared as a 1% solution in 50% ethanol, and alcian blue as a 1% solution in pure water. Afterwards, the sections were dehydrated through a series of increasing ethanol concentrations (50%, 75%, 96%) and mounted in Euparal. The slides were observed using a Zeiss Axio Imager.M2 compound microscope with an attached AxioCam MRc5 digital camera (Carl Zeiss). Images were analysed using ImageJ (Schneider et al. 2012), and anatomical traits (Table 1) were measured according to the recommendations of Scholz et al. (2013).

2.5.2 | *Transmission Electron Microscopy (TEM)*

Intervessel pit membrane thickness (T_{PM}; Table 1) was quantified on the same stem samples used for LM. Match-sized wood samples were kept as small as possible to ensure better fixation with glutaraldehyde 2.5% and formaldehyde 2% in a 0.1 M sodium cacodylate buffer (pH 7.2). They were rinsed three times in 0.1 M sodium cacodylate buffer, post-fixed with 1% buffered osmium tetroxide and cleaned again with buffer solution. Next, samples were stained with 1% uranyl acetate, dehydrated through increasing concentrations of ethanol (30%, 50%, 70%, 96% and twice in ≥ 99%) and embedded in Epon 812n (Electron Microscopy Sciences, Hatfield, England) for 48 h at 60°C in the oven. Trimming of Epon blocks into 2-μm-thick cross-sections was subsequently done using a rotary microtome with a glass knife to shape transverse surfaces with vessel-vessel contact areas. Subsequently, ultrathin (90–95 nm) sections were made using a Leica EM UC7 ultramicrotome with a diamond knife. Finally, these ultrathin sections were dried on film-coated copper slot grids with Formvar coating (Agar Scientific, Stansted, UK) and post-stained using uranyl acetate and lead citrate. Ultrastructural observations of intervessel pits were conducted using a transmission electron microscope JEM-1400 Plus (JEOL, Tokyo, Japan) equipped with an 11-megapixel camera (Quemesa, Olympus). T_{PM} was quantified by taking measurements at two different spots on each pit membrane using ImageJ (Schneider et al. 2012).

2.6 | Shared-Pot Drought Experiment

To assess how anatomical and functional traits in leaves and stems influence drought responses among *D. broteri* ploidies, we used a mixed-planting approach as described by Blackman et al. (2025). Twelve 1-year-old *D. broteri* individuals (three per ploidy level), previously grown in separate pots in the University of Tasmania glasshouse, were transplanted into three 10-L pots. Each pot contained one individual of each of the four ploidies. The pots were filled with a fine-textured 3:1 mixture of loam soil and potting mix, with added slow-release fertiliser. This soil type promotes strong root–soil contact and reduces hydraulic isolation during drought, helping to maintain similar soil water availability among neighbouring plants despite differences in individual size (Sperry et al. 1998; Hultine et al. 2006). Plants were watered daily for 1 month prior to the onset of the dry-down to allow substantial root overlap to develop within the shared soil, a condition shown to homogenise plant water status among individuals in mixed-planting experiments (Blackman et al. 2025). During this period, all individuals exhibited fully green canopies. The dry-down was initiated by withholding water, allowing soil moisture to gradually decline until individuals reached critical drought stress—defined as the point at which the first plant in each pot showed complete leaf senescence, which occurred after 20 days. At this point, the percentage of green canopy retention was visually estimated for each plant using close-range photographs, capturing differences among individuals in the extent of drought-induced leaf senescence.

2.7 | Statistical Analysis

Generalised linear models (GLMs) were used to assess the effect of ploidy (fixed factor: 2×, 4×, 6×, and 12×) on all measured anatomical and physiological variables. No random effects were

included in the models. The level of statistical significance was evaluated on a case-by-case basis, following the thresholds specified for each test in the text and figures where relevant. When a significant effect of ploidy was detected, Tukey's post hoc HSD tests were used to perform all pairwise comparisons among ploidy levels. Model residuals were assessed for normality using the Shapiro–Wilk test for each fitted model. Linear regressions were employed to examine correlations between leaf anatomical traits and T_{PM}-P_{25}, allowing analysis of stem structure–function relationships. All analyses and figures were produced using R v.4.4.1 (R Core Team 2024).

3 | Results

We detected highly coordinated changes in key functional leaf traits—cell size (area) and density of epidermal and vascular tissues—among cytotypes of *Dianthus broteri* (Figure 1). Stomatal size ranged from 555 to 1125 μm^2 and pavement cell size from 2275 to 5385 μm^2; these two traits were positively correlated ($R^2 = 0.48$, $p < 0.05$; Figure 1A). Although the densities of stomata and leaf veins varied to different extents (a fivefold change in stomatal density and a 1.4-fold change in vein density), they were strongly positively correlated as well ($R^2 = 0.59$, $p < 0.01$; Figure 1B). The well-established inverse relationship between stomatal size and density—driven by spatial constraints—was also observed, with smaller stomata occurring in leaves with higher stomatal densities ($R^2 = 0.41$, $p < 0.05$; Figure 1C).

Notably, the observed variation in leaf anatomical traits was significantly linked to ploidy level (Figures 2, S1). Higher-ploidy cytotypes tended to exhibit larger stomata and pavement cells (Figure 2A,B), coupled with reduced stomatal and vein densities (Figure 2C,D). While the second-highest ploidy level (6×) consistently differed from the 2× and 4×, the highest level (12×) slightly deviated from this trend. The 12× cytotype had significantly larger stomata than the 2× and 4× ($p < 0.05$; Figure 2A), but this was not accompanied by a consistent increase in pavement cell size ($p > 0.05$; Figure 2B) or by decreases in stomatal and vein densities ($p > 0.05$; Figure 2C,D).

Despite similar stomatal traits between higher-ploidy *D. broteri* 6× and 12× (Figures 2, S1), cuticular characteristics and g_{min} differed significantly, with the lower ploidy levels (2× and 4×) showing intermediate values. The 12× cytotype exhibited the thinnest epicuticular wax (lower T_{EW}; $p < 0.05$) and lowest T_p (Figures 3, S2), while 6× had both the highest T_{EW} and T_p (Figure 3). Regarding g_{min}, 12× showed consistently higher values within the pre–phase-transition range (25°C–33°C; 4.9 ± 0.2 mmol m^{-2} s^{-1}) compared with 2×, 4×, and 6× (2.4 ± 0.1, 1.8 ± 0.2, and 2.6 ± 0.2 mmol m^{-2} s^{-1}, respectively; $p < 0.05$; Figure 3).

Unlike leaf epidermal anatomy, the stem vasculature of *D. broteri* was not significantly affected by ploidy. Xylem tissue and cellular-level traits related to hydraulic safety remained stable across ploidy levels, with no changes in vessel lumen area (A_{VL}), wall thickness (T_V), theoretical implosion resistance ($(T_{VW}/D_{MAX})^2$), or grouping index (V_G; $p > 0.05$; Figures 4, S3).

This stem anatomical uniformity translated into similar stem hydraulic vulnerability across ploidies. Ploidy explained only 42% of the variation in stem P_{50}, which ranged from −1.83 to −3.79 MPa among the 12 individuals assessed (Figure 5A). Nevertheless, vulnerability curves revealed differences in embolism progression between cytotypes (Figure S4). This was reflected in P_{25}, which tended to occur at more negative water potentials in higher-ploidy individuals, indicating greater resistance to early embolism (Figure 5B). These plants, particularly 6× and 12×, were also characterised by greater intervessel pit membrane thickness (T_{PM}). T_{PM} was the only xylem anatomical trait that varied significantly with ploidy: on average, 6× and 12× exhibited T_{PM} values 66% higher than those of 2× and 4× ($p < 0.05$; Figures 5C, S5). These patterns converged in a significant negative T_{PM}-P_{25} relationship, with 6× and 12× cytotypes combining thicker intervessel pit membranes with more negative P_{25} (Figure 5D).

Despite similar P_{50} in stems—and even slightly more negative P_{25} values with increasing ploidy—the shared-pot experiment yielded one clear conclusion: *D. broteri* 12× was consistently the most affected cytotype in terms of canopy retention. All three 12× individuals completely lost their green, photosynthetic leaves by the end of the dry-down (Figure 6). In contrast, 2× and 6× individuals were significantly less affected by the imposed drought ($p < 0.05$; Figure 6), retaining on average $65.0 \pm 10.9\%$ and $82.8 \pm 11.3\%$ of their canopy, respectively.

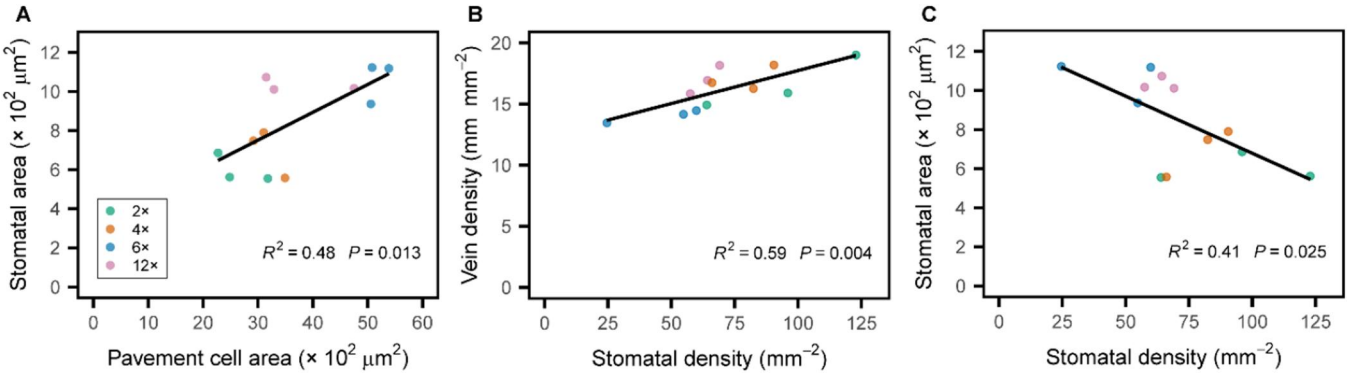

FIGURE 1 | Coordinated changes in leaf anatomical traits across the four ploidy levels (2×, 4×, 6×, and 12×) of *D. broteri*, shown in different colours. (A) Relationship between stomatal and pavement cell size. (B) Relationship between vein density and stomatal density. (C) Relationship between stomatal size and stomatal density. Linear regressions were all significant. [Color figure can be viewed at wileyonlinelibrary.com]

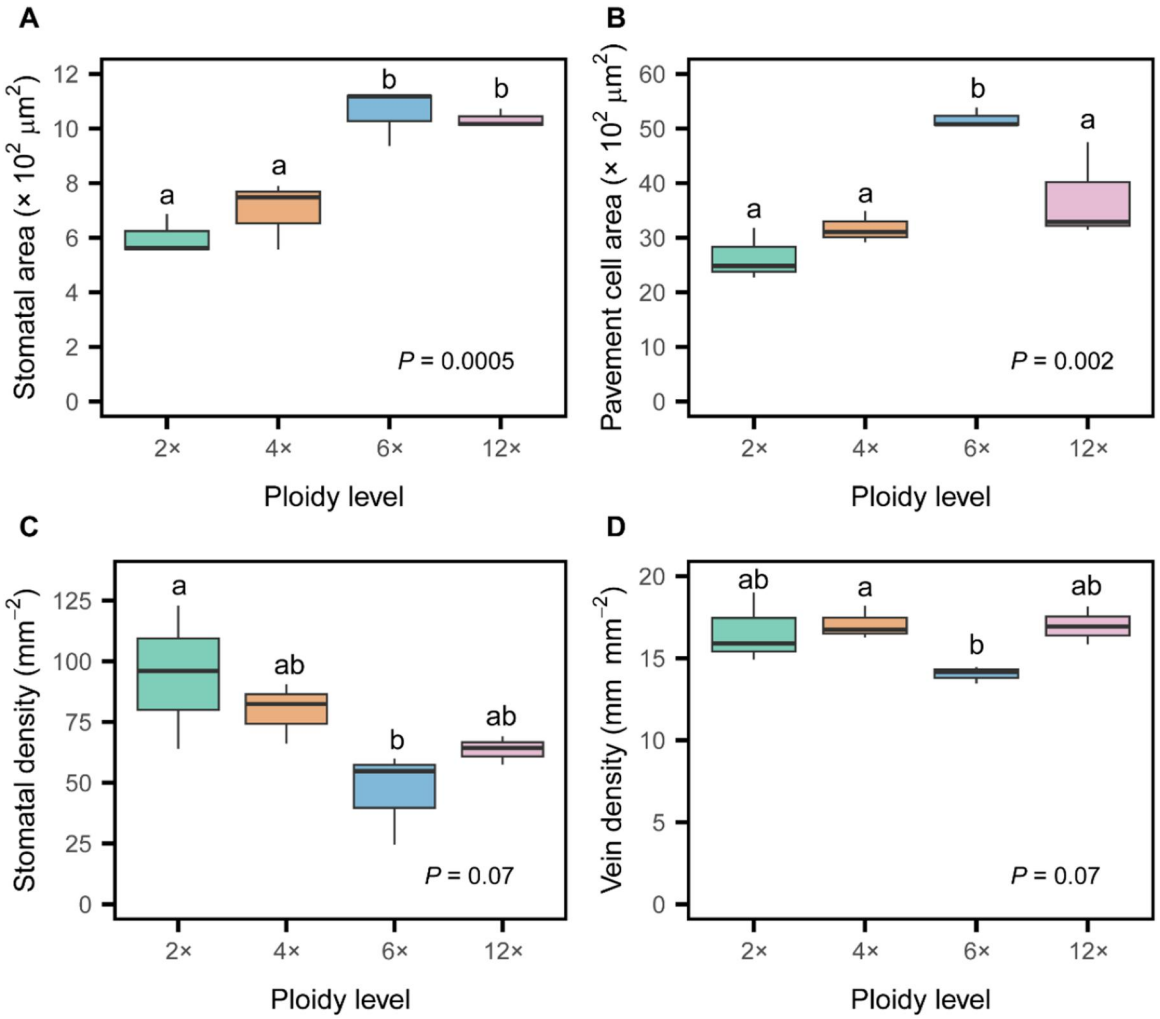

FIGURE 2 | Boxplots of leaf cell size and density across the four ploidy levels (2×, 4×, 6×, and 12×) of *D. broteri*. Shown are stomatal size (A), pavement cell size (B), stomatal density (C), and vein density (D). Horizontal lines indicate medians, boxes the interquartile range, and whiskers the non-outlier range. Different letters denote significant differences (GLM with Tukey's HSD, *p* values shown). [Color figure can be viewed at wileyonlinelibrary.com]

The 4× cytotype maintained 31.1 ± 41.6% green foliage, with two out of three individuals preserving functional leaf patches, and was not statistically different from any of the other cytotypes ($p > 0.05$; Figure 6).

4 | Discussion

4.1 | Leaf Anatomical Traits Scale With Ploidy and Are Coordinated to Support Leaf Function

As expected, in a within-species series spanning a sixfold genome multiplication from 2× to 12×, epidermal cells enlarged with increasing ploidy (Doyle and Coate 2019; Pacey et al. 2022). This correlation between ploidy and cell size is not necessarily driven by a direct biophysical mechanism, as a given genome size allows a wide range of mature cell volumes (Roddy et al. 2020). Stomatal spacing is not governed by geometry alone: cell types within the leaf epidermis compete for limited surface area, and stomatal density patterns may reflect developmental priorities rather than a hard packing limit (Baresch et al. 2019; Vieira-Goncalves and Roddy 2025). Nevertheless, our findings are broadly consistent with the 'passive dilution' mechanism, whereby increases in epidermal (pavement) cell size are accompanied by lower densities of veins and stomata due to spatial optimisation (Carins Murphy et al. 2016; Brodribb et al. 2017). This relationship, predicted by mathematical models linking epidermal cell area, stomatal dimensions and density, and maximum stomatal conductance (Sack and Buckley 2016), was retained in *D. broteri* up to the 6× cytotype (Figure 2). Such coordinated shifts in cell size across tissues may help preserve functional relationships regulating water delivery and loss (Brodribb et al. 2013), even in the presence of developmental challenges associated with polyploidy (Katagiri et al. 2016; Robinson et al. 2018). Supporting this interpretation, canopy and hydraulic conductance were recently found to covary tightly across ploidy levels in *D. broteri* (López-Jurado et al. 2025b).

Interestingly, with the additional duplication to 12×, large stomata co-occurred without a proportional decrease in stomatal or vein density, indicating that stomatal spacing is not strictly dictated by geometric limitations (Zhang et al. 2021). This pattern is consistent with observations that stomatal packing is

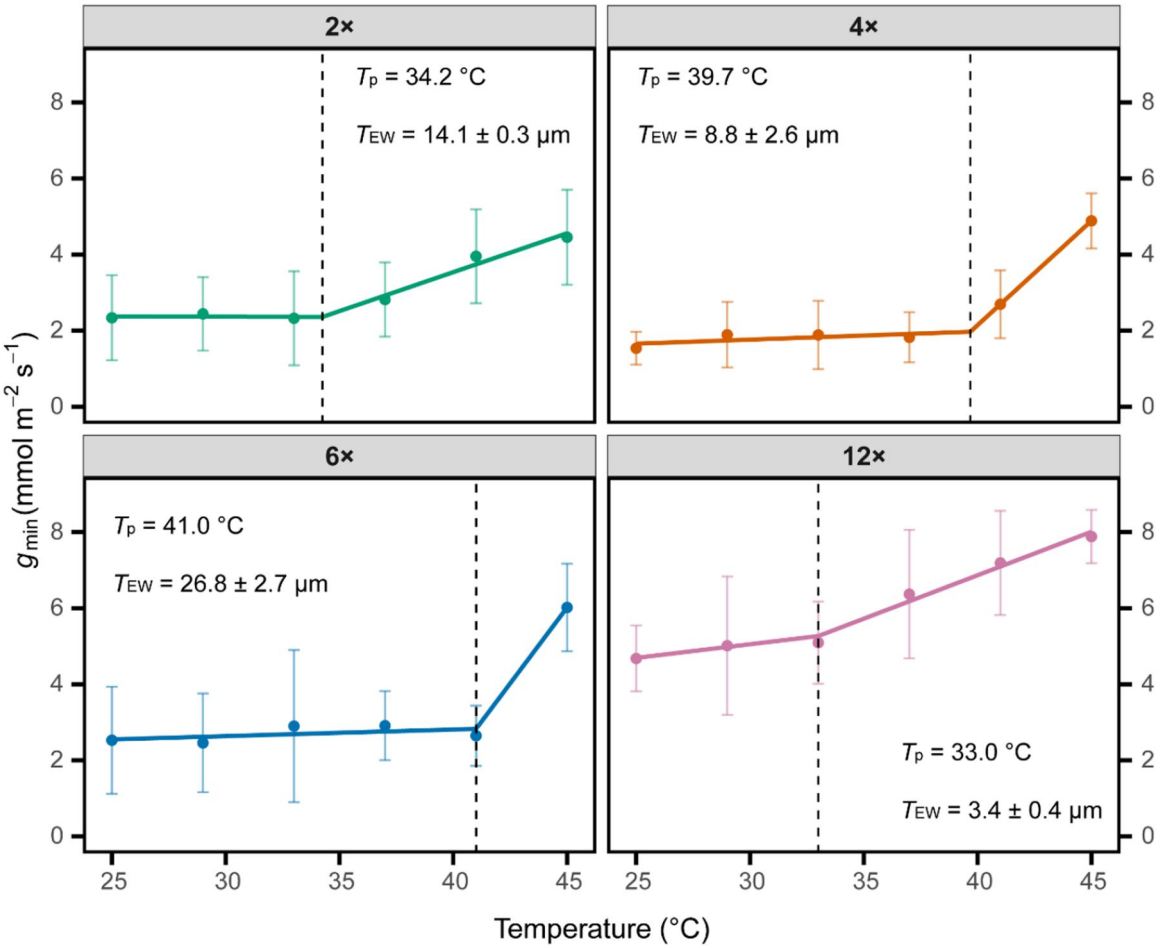

FIGURE 3 | Minimum leaf conductance to water vapour (g_{min}) across a temperature range in the four ploidy levels (2×, 4×, 6×, and 12×) of *D. broteri*. Values are means ± SE. Vertical dashed lines indicate the phase transition temperature (T_p), marking the breakpoint in the g_{min}–temperature relationship. The thickness of the leaf epicuticular wax layer (T_{EW}) is also shown for each ploidy. [Color figure can be viewed at wileyonlinelibrary.com]

more flexible in angiosperms than in pteridophytes or gymnosperms, and may be further relaxed in polyploids, which often exhibit altered gene expression (Spoelhof et al. 2017). In line with these traits, 12× *D. broteri* individuals have shown higher maximum stomatal conductance (López-Jurado et al. 2025b). The observed deviations from the expected ratios between leaf anatomical traits that regulate water supply and demand provide a mechanistic basis for a shift toward a productivity-maximising strategy in this ploidy.

4.2 | Stem Xylem Anatomy Is Conserved Across Ploidy, With Intervessel Pit Membrane Thickness Emerging as a Key Functional Trait

Despite the coordinated changes in leaf epidermal traits observed across ploidy levels, stem anatomy remained uniform. Ploidy had no detectable impact on vessel size (A_{VL}) or wall thickness (T_V and $(T_{VW}/D_{MAX})^2$), indicating that these traits linked to embolism resistance (Thonglim et al. 2021) are largely conserved as long as their key functional relationships with gas exchange are maintained. Although a handful of studies have examined stem xylem anatomy in relation to ploidy (Hao et al. 2013; Zhang et al. 2017; De Baerdemaeker et al. 2018; Barceló-Anguiano et al. 2021; Losada et al. 2023), this is still an open area of research as most ploidy-driven anatomical shifts documented in plants have focused on leaves (e.g., Van Laere et al. 2011; Baker et al. 2017; Tossi et al. 2022; Šmarda et al. 2023; Zhang et al. 2024a). The limited changes in vessel wall thickness across *D. broteri* cytotypes (Figure S3B, C) may be explained by the reduced deposition of lignin and cellulose in the secondary cell walls of polyploids relative to diploids (Corneillie et al. 2019), as observed in substantial parts of the wood cylinder in 6× and 12× (Figure 4). These two higher-level cytotypes also show stems with more pronounced secondary growth compared to 2× and 4× (Figure 4), which has been associated with increased embolism resistance in predominantly herbaceous angiosperm lineages (Dória et al. 2018, 2019). Likewise, porous intervessel pit membranes—primarily composed of layers of cellulose microfibrils (Kaack et al. 2019)—became markedly thicker with increasing ploidy (Figures 5C, S5). In fact, intervessel pit membrane thickness (T_{PM}) in 6× and 12× ploidies reached values above 1000 nm, exceeding the typical range reported for angiosperms (Jansen et al. 2009). Together, these patterns point to a resource-allocation trade-off in which cellulose investment may be redirected from secondary cell walls toward pit membranes in higher ploidies. This shift may also explain why T_V and T_{PM} in

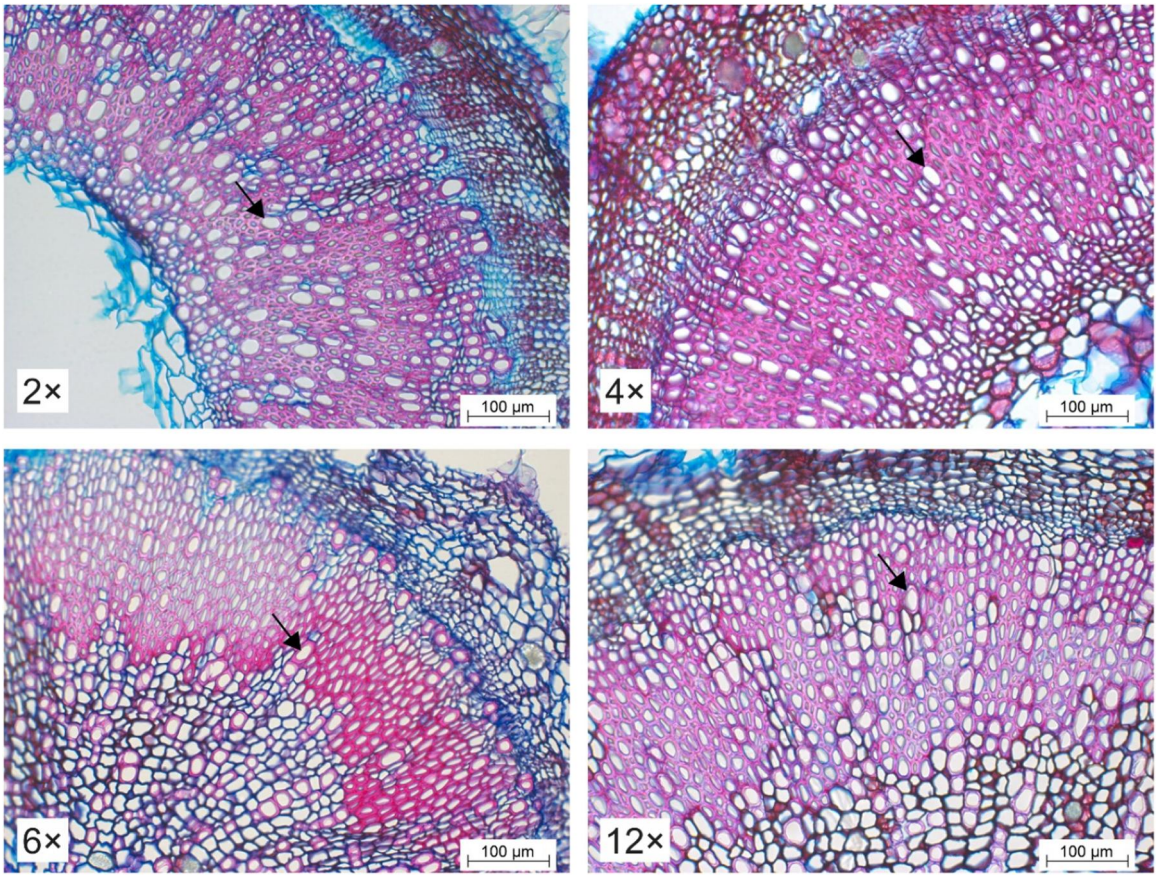

FIGURE 4 | Light microscopy images of cross-sections at the basal part of the main stem from representative samples of the four ploidy levels (2×, 4×, 6×, and 12×) of six-month-old *D. broteri* individuals. A scale bar is included in each panel and is identical across all images. Black arrows indicate individual xylem vessels. [Color figure can be viewed at wileyonlinelibrary.com]

D. broteri did not retain their previously described covariation (Jansen et al. 2009; Thonglim et al. 2021). To our knowledge, this is the first report of a ploidy-associated increase in T_{PM}, which is one of the main anatomical traits that show a consistent correlation with embolism resistance across a wide taxonomic range of angiosperms (Li et al. 2016; Lens et al. 2022). Such an important finding has significant implications for understanding stress resistance in plant polyploids and may inform future breeding and agronomic strategies.

However, in *Dianthus broteri*, the increase in T_{PM} did not translate into a safer overall hydraulic system (lower P_{50}) in higher ploidies. This suggests partial decoupling between conduit-level anatomy and whole-plant hydraulic safety, potentially reflecting altered trait coordination under polyploidy. Embolism resistance emerges from multiple anatomical and physicochemical drivers (Lens et al. 2022), and our P_{50} results are therefore likely explained by a combination of factors, including the distribution of conduit failure thresholds and the largest pore constrictions within interconduit pit membranes, rather than scaling proportionally with mean T_{PM} (Li et al. 2016; Kaack et al. 2021). Thick intervessel pit membranes—even in the lower ploidies of *D. broteri*—may nevertheless partially offset the potential hydraulic risks associated with high vessel connectivity (Johnson et al. 2020). All ploidies showed relatively elevated vessel grouping (V_G; Figure S3D) values, indicating a highly interconnected xylem network with multiple potential pathways for embolism spread. Such connectivity is generally linked to faster embolism progression leading to earlier hydraulic failure (Mrad et al. 2018; Wason et al. 2021). However, intervessel pit membranes act as safety barriers at each interconduit connection, regulating the movement of gas bubbles between adjacent vessels (Kaack et al. 2021; Zhang et al. 2024b). This function may be especially important during the early stages of drought, when most of the network remains functional, and embolism containment is more effective. As more vessels become embolized—each with numerous connections—the likelihood of embolism spread increases sharply (Wason et al. 2021; Roth-Nebelsick and Konrad 2024). This interpretation aligns with the delayed embolism spread observed in higher ploidies with thicker pit membranes, as indicated by their slightly lower P_{25} values (Figure 5B,C).

4.3 | Ploidy Levels Exhibit Contrasting Water-Use Syndromes Under Drought

The general trend in *D. broteri* across ploidy levels is that stem hydraulic safety is largely maintained (Figure 5A,B), while plant water status becomes more buffered with increasing ploidy during drought (López-Jurado et al. 2025b). However, this does not imply that higher-ploidy plants consistently outperform their lower-ploidy counterparts under all conditions. Instead,

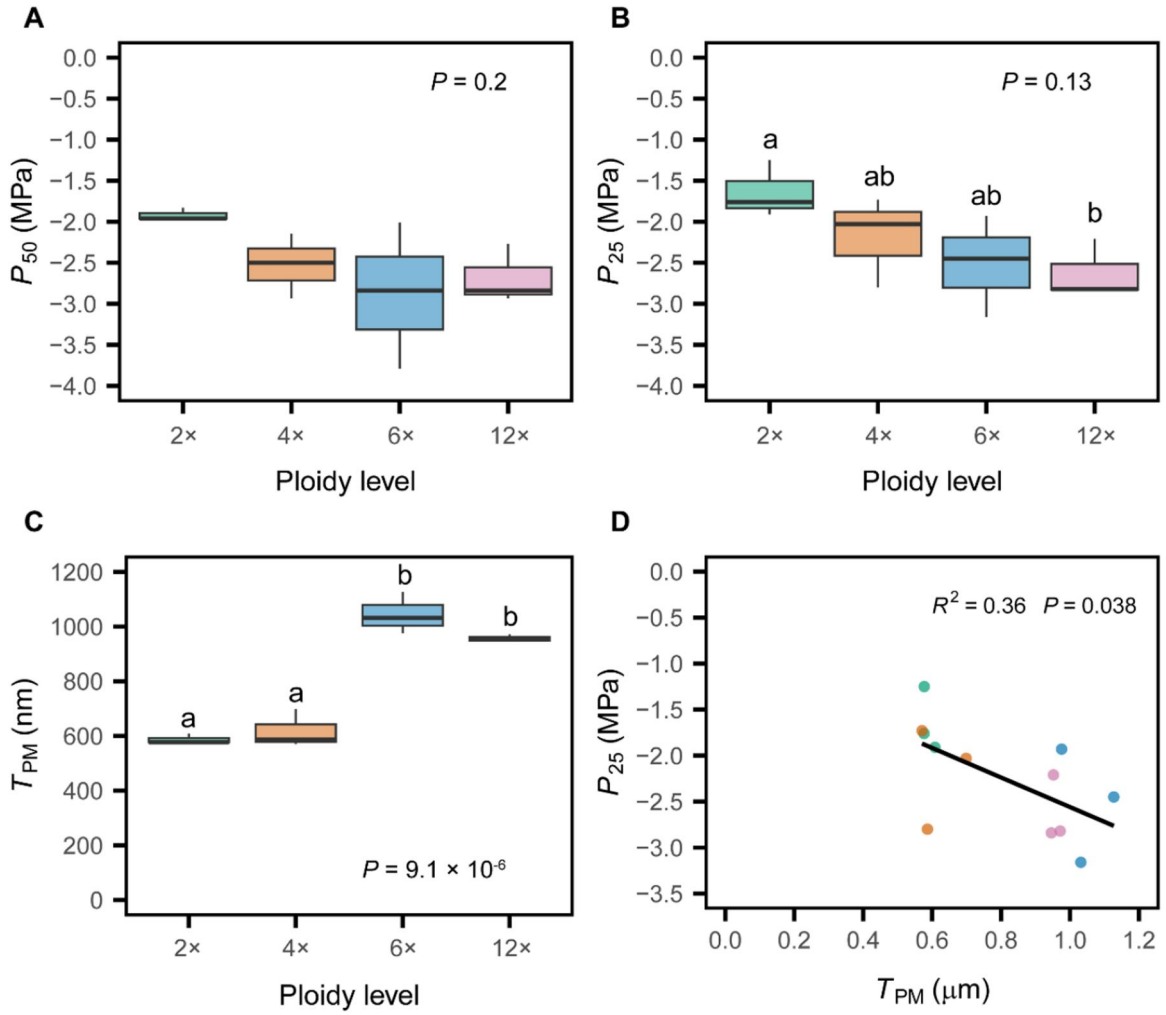

FIGURE 5 | Hydraulic vulnerability measurements and their relationship with intervessel pit membrane thickness (T_{PM}) in the four ploidy levels (2×, 4×, 6×, and 12×) of *D. broteri*. (A–C) Boxplots showing (A) xylem pressure inducing 50% loss of water transport (P_{50}), (B) water potential at P_{25}, and (C) T_{PM}. Different letters denote significant differences (GLM with Tukey's HSD, *p* values shown). (D) Scatterplot showing individual data points for the relationship between P_{25} and T_{PM}, with the linear regression indicated. Colours represent the four ploidy levels. [Color figure can be viewed at wileyonlinelibrary.com]

contrasting structure-function trait combinations among cytotypes reflect integrated water-use syndromes rather than a single unified drought response axis. The 2×, 4×, and 6× cytotypes exhibit traits associated with more conservative water use and reduced sensitivity to soil drying at both physiological and structural levels. Supporting this interpretation, the three lower ploidies showed a greater capacity to limit leaf water loss. They exhibited higher epicuticular wax deposition than the 12× cytotype (T_{EW}; Figure 3), which may contribute to their lower minimum leaf conductance (g_{min}; McAdam et al. 2025). In contrast, our data do not indicate a simple relationship between g_{min} and stomatal size or density across ploidies, differing from results reported in a multispecies study (Machado et al. 2021). For example, the 6× cytotype, despite having lower stomatal density and larger stomata than 2×, did not show lower g_{min}. As both ploidies fall within the lower range of stomatal trait values (Machado et al. 2021), this pattern may instead indicate differences in cuticle composition or structure that were not measured here (Bueno et al. 2019; Heredia et al. 2024). Interestingly, several drought tolerance traits become increasingly pronounced from 2× to 6×, arguably reflecting phenotypic innovations associated with polyploidy. In particular, 6× leaves exhibited the thickest and potentially most structurally stable wax layer, which reinforces cuticle impermeability and may contribute to their higher phase transition temperature (T_p; Burghardt and Riederer 2006; Bueno et al. 2019). This, in turn, promotes heat-drought resistance in this cytotype (Schuster et al. 2016), alongside its functionally tolerant photosynthetic system (López-Jurado et al. 2020). All these physiological and anatomical traits could help explain why 2×, 4×, and 6× plants showed significantly greater canopy retention following drought compared with 12× (Figure 6).

In contrast, the 12× cytotype showed large stomata and a thin epicuticular wax layer, coinciding with elevated g_{min} (Figure 3). Coupled with a lower T_p, 12× plants would be prone to greater water loss under high evaporative demand, increasing their vulnerability to rapid tissue dehydration (Cochard 2021). Disruption of water transport to the leaves can then trigger runaway cavitation, ultimately increasing the risk of irreversible tissue damage (Tonet et al. 2023). An apparent mitigation of this sensitivity to dehydration in the 12× cytotype is its ability to

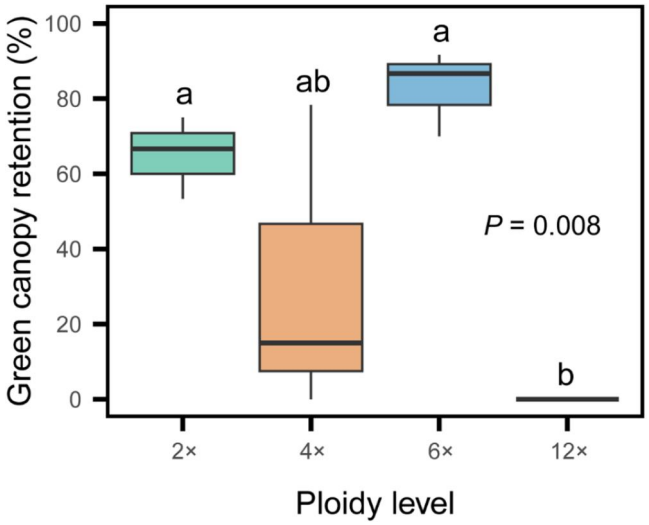

FIGURE 6 | Percentage of green leaf tissue retained after the shared-pot drought experiment in the four ploidy levels (2×, 4×, 6×, and 12×) of one-year-old *D. broteri* individuals. Different letters denote significant differences (GLM with Tukey's HSD, *p* value shown). [Color figure can be viewed at wileyonlinelibrary.com]

buffer declines in stem water potential due to enhanced water storage (López-Jurado et al. 2025b) and to delay the spread of xylem embolism, as reflected by its marginally lower P_{25} values than 2×. These trait combinations point to a high water-use behaviour in 12×, contrasting with the more conservative water use of lower-ploidy cytotypes.

Although stem xylem anatomical traits and P_{50} did not vary among ploidies, the lower leaf-to-root ratio and the maximum Huber value observed in 12× (López-Jurado et al. 2025b) indicate greater investment in stems and roots relative to leaves. This enhances essential plant structural support and a reliable water supply to the canopy, which in turn may underpin the persistence of this ploidy across seasonal climatic variations. Greater allocation to roots would also promote the exploration of larger soil volumes (Poorter et al. 2012) and enhance water storage, potentially serving as a major source for meeting the transpirational demands via hydraulic capacitance (McCarthy et al. 2025). Notably, the root-to-shoot ratio of 12× individuals has been reported to increase under elevated temperatures (López-Jurado et al. 2025a), suggesting plastic adjustment toward below-ground investment. In this regard, recent evidence has shown that the 12× cytotype outcompetes lower-ploidy cytotypes (2× and 4×) under low water availability (Rodríguez-Parra et al. 2025), indicating strong performance under soil moisture limitation despite contrasting aboveground responses. Consistent with this, 12× individuals showed widespread leaf senescence in the shared-pot experimental dry-down (Figure 6), although this response alone does not allow mechanistic distinction between active canopy reduction and hydraulically driven tissue loss. Field observations also report canopy loss during extreme hot-drought summers in this cytotype, followed by rapid post-drought canopy recovery (López-Jurado et al. 2019b). Taken together, trait-based, experimental, and field evidence suggest a seasonal drought response characterised by canopy turnover coupled with strong below-ground investment, rather than sustained leaf retention. This interpretation is further supported by reduced intrinsic growth rates in the 12× cytotype compared with lower ploidies (Rodríguez-Parra et al. 2025) and by its rapid, acquisitive behaviour inferred from leaf economic spectrum traits (López-Jurado et al. 2022).

5 | Conclusion

Here, we investigate how ploidy shapes plant–environment interactions, focusing on plant water relations, hydraulic vulnerability, and functional leaf and stem anatomy in the carnation *Dianthus broteri*, a species complex comprising diploid (2×), low-polyploid (4×), and high-polyploid (6× and 12×) cytotypes native to Spain and Portugal. Our study adds a new layer to the complex understanding of the biological consequences of polyploidy in plants. Vascular function was largely conserved among cytotypes, as xylem anatomical traits did not change with ploidy. However, we provide compelling empirical evidence that ploidy influenced cell size in the leaf epidermis, resulting in anatomical trait trade-offs in leaves that diverge from expected ratios between water supply and demand. These patterns highlight how a sixfold genome multiplication, together with distinct selective pressures acting on different organs depending on their role in water-use behaviour, shapes overall plant function. Integrating these findings with previous work on this species suggests that *D. broteri* cytotypes exhibit contrasting drought response strategies, rather than following a simple directional shift with increasing ploidy. Lower ploidies (2×, 4×, and particularly 6×) exhibit traits associated with more drought-tolerant behaviour, minimising water loss and maintaining an almost intact functional canopy after a period of water withholding. In contrast, the highest ploidy level (12×) experiences significant leaf loss under the same controlled drought conditions. However, greater investment in roots and stems may support seasonal leaf dieback and subsequent regrowth, potentially contributing to the protection of long-lived hydraulic tissues in its stressful native habitats. Reliance on this acquisitive water-use and canopy turnover strategy, however, could increase vulnerability under climate change. Taken together, these contrasting strategies suggest that shifts towards longer drought periods and higher atmospheric evaporative demand are likely to differentially filter cytotypes, favouring those with tighter control of water loss and sustained canopy function (2×–6×), while potentially limiting the persistence of highly acquisitive, high-ploidy forms (12×). Altogether, our findings support the view that these extreme ploidies are rare in nature not only due to genetic and reproductive constraints (e.g., meiotic irregularities, epigenetic instability; Comai 2005), but also because deviations from fundamental functional trade-offs can limit their establishment and survival in natural habitats.

Acknowledgements

We thank the University of Tasmania glasshouse team for their assistance and for providing facilities. We also acknowledge the technical support for microscopy work provided by R. Langelaan and B. Joan van Heuven at the Naturalis Biodiversity Center.

This study was made possible by visits of JLJ to the laboratories of TJB (Hobart, TAS, Australia) and FL (Leiden, the Netherlands), funded by the Research Plans of the Universidad de Sevilla, which also supported JLJ's predoctoral grant. Additional financial support was provided by

the ARC Centre of Excellence for Plant Success in Nature and Agriculture and the Research Project PGC2018-098358-B-I00 from the Spanish MICINN. This study was supported by the Universidad de Sevilla, Australian Research Council Centre of Excellence for Plant Success in Nature and Agriculture, and Ministerio de Ciencia e Innovación. Open access publishing facilitated by University of Tasmania, as part of the Wiley - University of Tasmania agreement via the Council of Australasian University Librarians.

Conflicts of Interest

The authors declare no conflicts of interest.

Data Availability Statement

The data that support the findings of this study are available from the corresponding author upon reasonable request.

References

De Baerdemaeker, N. J. F., N. Hias, J. Van Den Bulcke, W. Keulemans, and K. Steppe. 2018. "The Effect of Polyploidization on Tree Hydraulic Functioning." *American Journal of Botany* 105: 161–171.

Baker, R. L., Y. Yarkhunova, K. Vidal, B. E. Ewers, and C. Weinig. 2017. "Polyploidy and the Relationship Between Leaf Structure and Function: Implications for Correlated Evolution of Anatomy, Morphology, and Physiology in *Brassica*." *BMC Plant Biology* 17: 3.

Balao, F., R. Casimiro-Soriguer, M. Talavera, J. Herrera, and S. Talavera. 2009. "Distribution and Diversity of Cytotypes in *Dianthus Broteri* as Evidenced by Genome Size Variations." *Annals of Botany* 104: 965–973.

Balao, F., J. Herrera, and S. Talavera. 2011. "Phenotypic Consequences of Polyploidy and Genome Size at the Microevolutionary Scale: A Multivariate Morphological Approach." *New Phytologist* 192: 256–265.

Balao, F., S. Talavera, and J. Herrera. 2024. "Reproductive Ecology of *Dianthus Inoxianus*: A Rare Wild Carnation With a Specialized Pollination System." *Flora* 310: 152439.

Balao, F., L. M. Valente, P. Vargas, J. Herrera, and S. Talavera. 2010. "Radiative Evolution of Polyploid Races of the Iberian Carnation *Dianthus Broteri* (Caryophyllaceae)." *New Phytologist* 187: 542–551.

Barceló-Anguiano, M., N. M. Holbrook, J. I. Hormaza, and J. M. Losada. 2021. "Changes in Ploidy Affect Vascular Allometry and Hydraulic Function in *Mangifera Indica* Trees." *Plant Journal* 108: 541–554.

Baresch, A., C. Crifò, and C. K. Boyce. 2019. "Competition for Epidermal Space in the Evolution of Leaves With High Physiological Rates." *New Phytologist* 221: 628–639.

Barker, M. S., N. Arrigo, A. E. Baniaga, Z. Li, and D. A. Levin. 2016. "On the Relative Abundance of Autopolyploids and Allopolyploids." *New Phytologist* 210: 391–398.

Bielenberg, D. G. 2011. "Knowing When Not to Grow." *New Phytologist* 189: 3–5.

Blackman, C. J., T. J. Brodribb, and G. J. Jordan. 2010. "Leaf Hydraulic Vulnerability Is Related to Conduit Dimensions and Drought Resistance Across a Diverse Range of Woody Angiosperms." *New Phytologist* 188: 1113–1123.

Blackman, C. J., B. Halliwell, and T. J. Brodribb. 2025. "All Together Now: A Mixed-Planting Experiment Reveals Adaptive Drought Tolerance in Seedlings of 10 *Eucalyptus* Species." *Plant Physiology* 197: kiae632.

Bomblies, K. 2020. "When Everything Changes at Once: Finding a New Normal After Genome Duplication." *Proceedings of the Royal Society B: Biological Sciences* 287: 20202154.

Brodribb, T. J., and T. S. Feild. 2000. "Stem Hydraulic Supply Is Linked to Leaf Photosynthetic Capacity: Evidence From New Caledonian and Tasmanian Rainforests." *Plant, Cell & Environment* 23: 1381–1388.

Brodribb, T. J., G. J. Jordan, and R. J. Carpenter. 2013. "Unified Changes in Cell Size Permit Coordinated Leaf Evolution." *New Phytologist* 199: 559–570.

Brodribb, T. J., S. A. McAdam, and M. R. Carins Murphy. 2017. "Xylem and Stomata, Coordinated Through Time and Space." *Plant, Cell & Environment* 40: 872–880.

Brodribb, T. J., R. P. Skelton, S. A. M. McAdam, D. Bienaimé, C. J. Lucani, and P. Marmottant. 2016. "Visual Quantification of Embolism Reveals Leaf Vulnerability to Hydraulic Failure." *New Phytologist* 209: 1403–1409.

Brown, M. J. M., and G. J. Jordan. 2023. "No Cell Is an Island: Characterising the Leaf Epidermis Using Epidermalmorph, a New R Package." *New Phytologist* 237: 354–366.

Buck, A. L. 1981. "New Equations for Computing Vapor Pressure and Enhancement Factor." *Journal of Applied Meteorology* 20: 1527–1532.

Bueno, A., A. Alfarhan, K. Arand, et al. 2019. "Effects of Temperature on the Cuticular Transpiration Barrier of Two Desert Plants With Water-Spender and Water-Saver Strategies." *Journal of Experimental Botany* 70: 1613–1625.

Burghardt, M., and M. Riederer. 2006. "Cuticular Transpiration." In *Biology of the Plant Cuticle*, edited by M. Riederer and C. Müller, 292–311. Oxford, UK: Blackwell Publishing Ltd.

Carins Murphy, M. R., G. J. Jordan, and T. J. Brodribb. 2016. "Cell Expansion Not Cell Differentiation Predominantly Co-Ordinates Veins and Stomata Within and Among Herbs and Woody Angiosperms Grown Under Sun and Shade." *Annals of Botany* 118: 1127–1138.

Cochard, H. 2021. "A New Mechanism for Tree Mortality Due to Drought and Heatwaves." *Peer Community Journal* 1: e36.

Comai, L. 2005. "The Advantages and Disadvantages of Being Polyploid." *Nature Reviews Genetics* 6: 836–846.

Corneillie, S., N. De Storme, R. Van Acker, et al. 2019. "Polyploidy Affects Plant Growth and Alters Cell Wall Composition." *Plant Physiology* 179: 74–87.

Dória, L. C., C. Meijs, D. S. Podadera, et al. 2019. "Embolism Resistance in Stems of Herbaceous Brassicaceae and Asteraceae Is Linked to Differences in Woodiness and Precipitation." *Annals of Botany* 124: 1–14.

Dória, L. C., D. S. Podadera, M. Del Arco, et al. 2018. "Insular Woody Daisies (*Argyranthemum*, Asteraceae) Are More Resistant to Drought-Induced Hydraulic Failure Than Their Herbaceous Relatives." *Functional Ecology* 32: 1467–1478.

Doyle, J. J., and J. E. Coate. 2019. "Polyploidy, the Nucleotype, and Novelty: The Impact of Genome Doubling on the Biology of the Cell." *International Journal of Plant Sciences* 180: 1–52.

Duursma, R., and B. Choat. 2017. "Fitplc - An R Package to Fit Hydraulic Vulnerability Curves." *Journal of Plant Hydraulics* 4: e002.

Duursma, R. A., C. J. Blackman, R. Lopéz, N. K. Martin-StPaul, H. Cochard, and B. E. Medlyn. 2019. "On the Minimum Leaf Conductance: Its Role in Models of Plant Water Use, and Ecological and Environmental Controls." *New Phytologist* 221: 693–705.

Ebadi, M., Q. Bafort, E. Mizrachi, et al. 2023. "The Duplication of Genomes and Genetic Networks and Its Potential for Evolutionary Adaptation and Survival During Environmental Turmoil." *Proceedings of the National Academy of Sciences* 120: e2307289120.

Folk, R. A., C. M. Siniscalchi, and D. E. Soltis. 2020. "Angiosperms at the Edge: Extremity, Diversity, and Phylogeny." *Plant, Cell & Environment* 43: 2871–2893.

Gleason, S. M., M. Westoby, S. Jansen, et al. 2016. "On Research Priorities to Advance Understanding of the Safety–Efficiency Tradeoff in Xylem: A Response to Bittencourt et al.'s (2016) Comment 'On Xylem Hydraulic Efficiencies, Wood Space-Use and the Safety–Efficiency Tradeoff." *New Phytologist* 211: 1156–1158.

Greer, B. T., C. Still, G. L. Cullinan, J. R. Brooks, and F. C. Meinzer. 2018. "Polyploidy Influences Plant–Environment Interactions in Quaking Aspen (*Populus Tremuloides* Michx.)." *Tree Physiology* 38: 630–640.

Grossiord, C., D. E. M. Ulrich, and A. Vilagrosa. 2020. "Controls of the Hydraulic Safety–Efficiency Trade-Off." *Tree Physiology* 40: 573–576.

Hao, G. Y., M. E. Lucero, S. C. Sanderson, E. H. Zacharias, and N. M. Holbrook. 2013. "Polyploidy Enhances the Occupation of Heterogeneous Environments Through Hydraulic Related Trade-Offs in *Atriplex Canescens* (Chenopodiaceae)." *New Phytologist* 197: 970–978.

Heredia, A., J. J. Benítez, A. González Moreno, and E. Domínguez. 2024. "Revisiting Plant Cuticle Biophysics." *New Phytologist* 244: 65–73.

Hultine, K. R., D. F. Koepke, W. T. Pockman, A. Fravolini, J. S. Sperry, and D. G. Williams. 2006. "Influence of Soil Texture on Hydraulic Properties and Water Relations of a Dominant Warm-Desert Phreatophyte." *Tree Physiology* 26: 313–323.

Jansen, S., B. Choat, and A. Pletsers. 2009. "Morphological Variation of Intervessel Pit Membranes and Implications to Xylem Function in Angiosperms." *American Journal of Botany* 96: 409–419.

Johnson, K. M., C. Brodersen, M. R. Carins-Murphy, B. Choat, and T. J. Brodribb. 2020. "Xylem Embolism Spreads by Single-Conduit Events in Three Dry Forest Angiosperm Stems." *Plant Physiology* 184: 212–222.

Kaack, L., C. M. Altaner, C. Carmesin, et al. 2019. "Function and Three-Dimensional Structure of Intervessel Pit Membranes in Angiosperms: A Review." *IAWA Journal* 40: 673–702.

Kaack, L., M. Weber, E. Isasa, et al. 2021. "Pore Constrictions in Intervessel Pit Membranes Provide a Mechanistic Explanation for Xylem Embolism Resistance in Angiosperms." *New Phytologist* 230: 1829–1843.

Katagiri, Y., J. Hasegawa, U. Fujikura, R. Hoshino, S. Matsunaga, and H. Tsukaya. 2016. "The Coordination of Ploidy and Cell Size Differs Between Cell Layers in Leaves." *Development* 143: 1120–1125.

Van Laere, K., S. C. França, H. Vansteenkiste, J. Van Huylenbroeck, K. Steppe, and M. C. Van Labeke. 2011. "Influence of Ploidy Level on Morphology, Growth and Drought Susceptibility in *Spathiphyllum Wallisii*." *Acta Physiologiae Plantarum* 33: 1149–1156.

Lens, F., S. M. Gleason, G. Bortolami, C. Brodersen, S. Delzon, and S. Jansen. 2022. "Functional Xylem Characteristics Associated With Drought-Induced Embolism in Angiosperms." *New Phytologist* 236: 2019–2036.

Lens, F., S. M. Gleason, G. Bortolami, C. Brodersen, S. Delzon, and S. Jansen. 2023. "Comparative Anatomy Vs Mechanistic Understanding: How to Interpret the Diameter-Vulnerability Link." *IAWA Journal* 44: 368–380.

Lens, F., A. Tixier, H. Cochard, J. S. Sperry, S. Jansen, and S. Herbette. 2013. "Embolism Resistance as a Key Mechanism to Understand Adaptive Plant Strategies." *Current Opinion in Plant Biology* 16: 287–292.

Li, S., F. Lens, S. Espino, et al. 2016. "Intervessel Pit Membrane Thickness as a Key Determinant of Embolism Resistance in Angiosperm Xylem." *IAWA Journal* 37: 152–171.

López-Jurado, J., F. Balao, and E. Mateos-Naranjo. 2020. "Polyploidy-Mediated Divergent Light-Harvesting and Photoprotection Strategies Under Temperature Stress in a Mediterranean Carnation Complex." *Environmental and Experimental Botany* 171: 103956.

López-Jurado, J., F. Balao, and E. Mateos-Naranjo. 2025a. "Impacts of Elevated Temperature and CO_2 Concentration on Carbon Metabolism in An Endangered Carnation: Consequences for Biomass Allocation and Flowering." *Plant Physiology and Biochemistry* 221: 109617.

López-Jurado, J., I. Bourbia, and T. J. Brodribb. 2025b. "Polyploidy Drives Changes in Tissue Allocation Modifying Whole-Plant Water Relations." *Plant Physiology* 197: kiaf079.

López-Jurado, J., E. Mateos-Naranjo, J. L. García-Castaño, and F. Balao. 2019b. "Conditions for Translocation of a Key Threatened Species, *Dianthus Inoxianus* Gallego, in the Southwestern Iberian Mediterranean Forest." *Forest Ecology and Management* 446: 1–9.

López-Jurado, J., E. Mateos-Naranjo, and F. Balao. 2019a. "Niche Divergence and Limits to Expansion in the High Polyploid *Dianthus Broteri* Complex." *New Phytologist* 222: 1076–1087.

López-Jurado, J., E. Mateos-Naranjo, and F. Balao. 2022. "Polyploidy Promotes Divergent Evolution Across the Leaf Economics Spectrum and Plant Edaphic Niche in the *Dianthus Broteri* Complex." *Journal of Ecology* 110: 605–618.

Losada, J. M., N. Blanco-Moure, A. Fonollá, E. Martínez-Ferrí, and J. I. Hormaza. 2023. "Hydraulic Tradeoffs Underlie Enhanced Performance of Polyploid Trees Under Soil Water Deficit." *Plant Physiology* 192: 1821–1835.

Machado, R., L. Loram-Lourenço, F. S. Farnese, et al. 2021. "Where Do Leaf Water Leaks Come From? Trade-Offs Underlying the Variability in Minimum Conductance Across Tropical Savanna Species With Contrasting Growth Strategies." *New Phytologist* 229: 1415–1430.

Maherali, H., A. E. Walden, and B. C. Husband. 2009. "Genome Duplication and the Evolution of Physiological Responses to Water Stress." *New Phytologist* 184: 721–731.

Manzoni, S., G. Vico, G. Katul, S. Palmroth, R. B. Jackson, and A. Porporato. 2013. "Hydraulic Limits on Maximum Plant Transpiration and the Emergence of the Safety–Efficiency Trade-Off." *New Phytologist* 198: 169–178.

Martin-StPaul, N., S. Delzon, and H. Cochard. 2017. "Plant Resistance to Drought Depends on Timely Stomatal Closure." *Ecology Letters* 20: 1437–1447.

McAdam, S. A. M., C. A. Baker, C. N. Kane, et al. 2025. "Tracking the Paths of Residual Conductance During Leaf Expansion in *Tilia Americana* and *Fagus Grandifolia*." *Plant Physiology* 199: kiaf150.

McCarthy, C., I. Bourbia, and T. Brodribb. 2025. "Substantial Capacitance Found in the Roots of 2 Contrasting Conifer Species." *Plant Physiology* 198: kiaf116.

McDowell, N., W. T. Pockman, C. D. Allen, et al. 2008. "Mechanisms of Plant Survival and Mortality During Drought: Why Do Some Plants Survive While Others Succumb to Drought?" *New Phytologist* 178: 719–739.

McKown, A. D., H. Cochard, and L. Sack. 2010. "Decoding Leaf Hydraulics With a Spatially Explicit Model: Principles of Venation Architecture and Implications for Its Evolution." *American Naturalist* 175: 447–460.

Meirmans, P. G., and F. Kolář. 2025. "Whole-Genome Duplication Leads to Significant but Inconsistent Changes in Climatic Niche." *Proceedings of the National Academy of Sciences* 122: e2424785122.

Messier, J., B. J. McGill, B. J. Enquist, and M. J. Lechowicz. 2017. "Trait Variation and Integration Across Scales: Is the Leaf Economic Spectrum Present at Local Scales?" *Ecography* 40: 685–697.

Mrad, A., J. Domec, C. Huang, F. Lens, and G. Katul. 2018. "A Network Model Links Wood Anatomy to Xylem Tissue Hydraulic Behaviour and Vulnerability to Cavitation." *Plant, Cell & Environment* 41: 2718–2730.

Muggeo, V. M. R. 2008. "Segmented: An R Package to Fit Regression Models With Broken-Line Relationships." *R News* 8: 20–25.

Otto, S. P., and J. Whitton. 2000. "Polyploid Incidence and Evolution." *Annual Review of Genetics* 34: 401–437.

Pacey, E. K., H. Maherali, and B. C. Husband. 2022. "Polyploidy Increases Storage but Decreases Structural Stability in *Arabidopsis Thaliana*." *Current Biology* 32: 4057–4063.e3.

Van De Peer, Y., T.-L. Ashman, P. S. Soltis, and D. E. Soltis. 2021. "Polyploidy: An Evolutionary and Ecological Force in Stressful Times." *Plant Cell* 33: 11–26.

Van De Peer, Y., E. Mizrachi, and K. Marchal. 2017. "The Evolutionary Significance of Polyploidy." *Nature Reviews Genetics* 18: 411–424.

Poorter, H., K. J. Niklas, P. B. Reich, J. Oleksyn, P. Poot, and L. Mommer. 2012. "Biomass Allocation to Leaves, Stems and Roots: Meta-Analyses of Interspecific Variation and Environmental Control." *New Phytologist* 193: 30–50.

Preisler, Y., T. Hölttä, J. M. Grünzweig, et al. 2022. "The Importance of Tree Internal Water Storage Under Drought Conditions." *Tree Physiology* 42: 771–783.

R Core Team. (2024) R: A Language and Environment for Statistical Computing. R Foundation for Statistical Computing, Vienna, Austria.

Rice, A., P. Šmarda, M. Novosolov, et al. 2019. "The Global Biogeography of Polyploid Plants." *Nature Ecology & Evolution* 3: 265–273.

Robinson, D. O., J. E. Coate, A. Singh, et al. 2018. "Ploidy and Size at Multiple Scales in the *Arabidopsis* Sepal." *Plant Cell* 30: 2308–2329.

Roddy, A. B., G. Théroux-Rancourt, T. Abbo, et al. 2020. "The Scaling of Genome Size and Cell Size Limits Maximum Rates of Photosynthesis With Implications for Ecological Strategies." *International Journal of Plant Sciences* 181: 75–87.

Rodriguez-Dominguez, C. M., A. Forner, S. Martorell, et al. 2022. "Leaf Water Potential Measurements Using the Pressure Chamber: Synthetic Testing of Assumptions Towards Best Practices for Precision and Accuracy." *Plant, Cell & Environment* 45: 2037–2061.

Rodríguez-Parra, A., J. López-Jurado, E. Mateos-Naranjo, and F. Balao. 2025. "Functional Traits and Soil Water Availability Shape Competitive Interactions in a Diploid–Polyploid Complex." *Journal of Ecology* 113: 2332–2345.

Roth-Nebelsick, A., and W. Konrad. 2024. "Modeling and Analyzing Xylem Vulnerability to Embolism as an Epidemic Process." In Xylem. *Methods in Molecular Biology*, edited by J. Agusti, 17–34. New York, NY: Springer US.

Sack, L., and T. N. Buckley. 2016. "The Developmental Basis of Stomatal Density and Flux." *Plant Physiology* 171: 2358–2363.

Schippers, J. H. M., R. Schmidt, C. Wagstaff, and H.-C. Jing. 2015. "Living to Die and Dying to Live: The Survival Strategy Behind Leaf Senescence." *Plant Physiology* 169: 914–930.

Schneider, C. A., W. S. Rasband, and K. W. Eliceiri. 2012. "NIH Image to Imagej: 25 Years of Image Analysis." *Nature Methods* 9: 671–675.

Scholz, A., M. Klepsch, Z. Karimi, and S. Jansen. 2013. "How to Quantify Conduits in Wood?" *Frontiers in Plant Science* 4: 56.

Schuster, A.-C., M. Burghardt, A. Alfarhan, et al. 2016. "Effectiveness of Cuticular Transpiration Barriers in a Desert Plant at Controlling Water Loss at High Temperatures." *AoB Plants* 8: plw027.

Shao, J., X. Zhou, P. Zhang, et al. 2023. "Embolism Resistance Explains Mortality and Recovery of Five Subtropical Evergreen Broadleaf Trees to Persistent Drought." *Ecology* 104: e3877.

Slot, M., T. Nardwattanawong, G. G. Hernández, A. Bueno, M. Riederer, and K. Winter. 2021. "Large Differences in Leaf Cuticle Conductance and Its Temperature Response Among 24 Tropical Tree Species From Across a Rainfall Gradient." *New Phytologist* 232: 1618–1631.

Soltis, P. S., and D. E. Soltis. 2016. "Ancient WGD Events as Drivers of Key Innovations in Angiosperms." *Current Opinion in Plant Biology* 30: 159–165.

Sperry, J. S., F. R. Adler, G. S. Campbell, and J. P. Comstock. 1998. "Limitation of Plant Water Use by Rhizosphere and Xylem Conductance: Results From a Model." *Plant, Cell & Environment* 21: 347–359.

Spoelhof, J. P., P. S. Soltis, and D. E. Soltis. 2017. "Pure Polyploidy: Closing the Gaps in Autopolyploid Research." *Journal of Systematics and Evolution* 55: 340–352.

Stebbins, G. L. 1971. *Chromosomal Evolution in Higher Plants*. London: Edward Arnold Ltd.

Thonglim, A., S. Delzon, M. Larter, et al. 2021. "Intervessel Pit Membrane Thickness Best Explains Variation in Embolism Resistance Amongst Stems of *Arabidopsis Thaliana* Accessions." *Annals of Botany* 128: 171–182.

Tonet, V., M. Carins-Murphy, R. Deans, and T. J. Brodribb. 2023. "Deadly Acceleration in Dehydration of *Eucalyptus Viminalis* Leaves Coincides With High-Order Vein Cavitation." *Plant Physiology* 191: 1648–1661.

Tossi, V. E., L. J. Martínez Tosar, L. E. Laino, et al. 2022. "Impact of Polyploidy on Plant Tolerance to Abiotic and Biotic Stresses." *Frontiers in Plant Science* 13: 869423.

Trojak-Goluch, A., M. Kawka-Lipińska, K. Wielgusz, and M. Praczyk. 2021. "Polyploidy in Industrial Crops: Applications and Perspectives in Plant Breeding." *Agronomy* 11: 2574.

Vieira-Goncalves, D., and A. B. Roddy. 2025. "Developmental Changes in Epidermal Anatomy, Drought Tolerance and Biomechanics in the Leaves of a Tropical Fern." *Annals of Botany* 136: 1641–1651.

Volaire, F. 2018. "A Unified Framework of Plant Adaptive Strategies to Drought: Crossing Scales and Disciplines." *Global Change Biology* 24: 2929–2938.

Wason, J., M. Bouda, E. F. Lee, et al. 2021. "Xylem Network Connectivity and Embolism Spread in Grapevine (*Vitis Vinifera* L." *Plant Physiology* 186: 373–387.

Wood, T. E., N. Takebayashi, M. S. Barker, I. Mayrose, P. B. Greenspoon, and L. H. Rieseberg. 2009. "The Frequency of Polyploid Speciation in Vascular Plants." *Proceedings of the National Academy of Sciences* 106: 13875–13879.

Yan, C.-L., M.-Y. Ni, K.-F. Cao, and S.-D. Zhu. 2020. "Leaf Hydraulic Safety Margin and Safety–Efficiency Trade-Off Across Angiosperm Woody Species." *Biology Letters* 16: 20200456.

Zhang, J., C. Cheng, F. Xiao, et al. 2024a. "Effects of Ploidy Level on Leaf Morphology, Stomata, and Anatomical Structure of *Hibiscus Syriacus* L." *BMC Plant Biology* 24: 1133.

Zhang, L., S. Wang, X. Yang, X. Cui, and H. Niu. 2021. "An Intrinsic Geometric Constraint on Morphological Stomatal Traits." *Frontiers in Plant Science* 12: 658702.

Zhang, L., S. Wu, X. Chang, et al. 2020. "The Ancient Wave of Polyploidization Events in Flowering Plants and Their Facilitated Adaptation to Environmental Stress." *Plant, Cell & Environment* 43: 2847–2856.

Zhang, W.-W., J. Song, M. Wang, et al. 2017. "Divergences in Hydraulic Architecture Form an Important Basis for Niche Differentiation Between Diploid and Polyploid *Betula* Species in NE China." *Tree Physiology* 37: 604–616.

Zhang, Y., L. Pereira, L. Kaack, J. Liu, and S. Jansen. 2024b. "Gold Perfusion Experiments Support the Multi-Layered, Mesoporous Nature of Intervessel Pit Membranes in Angiosperm Xylem." *New Phytologist* 242: 493–506.

Zimmermann, M. H. 1983. *Xylem Structure and the Ascent of Sap*. Berlin, Heidelberg: Springer-Verlag.

Šímová, I., and T. Herben. 2012. "Geometrical Constraints in the Scaling Relationships Between Genome Size, Cell Size and Cell Cycle Length in Herbaceous Plants." *Proceedings of the Royal Society B: Biological Sciences* 279: 867–875.

Šmarda, P., K. Klem, O. Knápek, et al. 2023. "Growth, Physiology, and Stomatal Parameters of Plant Polyploids Grown Under Ice Age, Present-Day, and Future Co_2 Concentrations." *New Phytologist* 239: 399–414.

Supporting Information

Additional supporting information can be found online in the Supporting Information section.

Figure S1: Light microscopy images of the leaf cuticle in *D. broteri* ploidies.
Figure S2: Light microscopy images of leaf epicuticular wax in *D. broteri* ploidies.
Figure S3: Stem xylem anatomical traits from light microscopy cross-sections in *D. broteri* ploidies.
Figure S4: Stem vulnerability curves in *D. broteri* ploidies.
Figure S5: Transmission electron microscopy images of intervessel pit membranes in *D. broteri* ploidies.
Table S1: Climatic characteristics of the sampled *D. broteri* populations.